Influence of Charge and Polarity on the Redox Potentials of High-Potential Iron−Sulfur Proteins: Evidence for the Existence of Two Groups†

H. A. Heering,‡ Y. B. M. Bulsink,‡ W. R. Hagen,*,‡ and T. E. Meyer§

Department of Biochemistry, Agricultural University Wageningen, NL-6703 HA Wageningen, The Netherlands, and Department of Biochemistry, University of Arizona, Tucson, Arizona 85721

Received April 4, 1995; Revised Manuscript Received August 16, 1995⊗

ABSTRACT: We have investigated the HiPIPs from *Ectothiorhodospira vacuolata* (iso-1 and iso-2), *Chromatium vinosum*, *Rhodocyclus gelatinosus*, *Rhodocyclus tenuis* (strain 2761), *Rhodopila globiformis*, and *Rhodospirillum salinarum* (iso-2) by direct electrochemistry. Using a glassy carbon electrode with a negatively charged surface, direct, unpromoted electrochemistry is possible with the positively charged HiPIPs. With the negatively charged HiPIPs, the positively charged and flexible bridging promoter poly(L-lysine) is required. The stability of the response can be improved by morpholin, aspartate, tryptophan, or 4,4′-dipyridyl. These "stabilizers" prevent the blocking of the electrode by denatured protein. The redox potential of 500 mV found for *R. salinarum* iso-2 is the highest HiPIP potential reported. The presence of histidines in the sequence does not *per se* predict a pH-dependent redox potential. Only *C. vinosum* and *R. gelatinosus* HiPIPs show a weak but significant pH dependence with a difference of 35 mV between the low- and the high-pH form and maximum slopes of −20 mV/unit. The dependence of the midpoint potential on temperature and on ionic strength varies over the different HiPIPs. The dependence of the potentials on $\sqrt{I}$ cannot be fully explained by the Debye−Hückel theory because the linearity exceeds the limiting concentration and only small negative slopes are observed (0 to −28 mV/$\sqrt{M}$). Combination of the sequences, the optical spectra, the overall charges, and the redox thermodynamics suggests the existence of two groups of HiPIPs. One group consists of *Chromatium*-like HiPIPs with redox potentials between 300 and 350 mV, modulated only by the solvation of the cluster. The second group is formed by *Ectothiorhodospira*-like HiPIPs with potentials between 50 and 500 mV, modulated by the overall charge of the peptide (25 mV/unit) and by the solvation of the cluster.

The high-potential iron−sulfur proteins form a group of related and well-studied small redox proteins (6−10 kDa) (Bartsch, 1978; Meyer, 1994).[1] They form a special class of ferredoxins, containing a [4Fe-4S] cluster coordinated by four cysteinyl sulfur ligands and buried in a hydrophobic environment. Most HiPIPs are found in purple photosynthetic bacteria, but a HiPIP is also present in a halophilic, denitrifying *Paracoccus* species (Bartsch, 1991; Tedro *et al.*, 1977). The primary structures of many HiPIPs have been determined (see Table 1 for references), and the crystal structures of the HiPIPs from *Chromatium vinosum*, *Rhodocyclus tenuis* strain 2761, *Ectothiorhodospira halophila* (iso-1), and *Ectothiorhodospira vacuolata* (iso-2) are known (Carter *et al.*, 1974a; Freer *et al.*, 1975; Breiter *et al.*, 1991; Rayment *et al.*, 1992; Benning *et al.*, 1994). For *Ectothiorhodospira halophila* iso-2, a molecular dynamics model structure has been calculated (Banci *et al.*, 1993a), and NMR structures have been reported for *E. halophila* iso-2 and for *C. vinosum* (Banci *et al.*, 1994, 1995). Although the homology of the sequences is low, the structural homology is high, especially around the cluster. There are however differences in the electronic structures of the $[4Fe\text{-}4S]^{3+}$ clusters (Nettesheim *et al.*, 1992; Banci *et al.*, 1993a,b; Bertini *et al.*, 1992, 1993). A synthetic gene encoding the *E. halophila* iso-1 HiPIP has been expressed in *Escherichia coli* (Eltis *et al.*, 1994).

Crystallography and resonance Raman studies show that the structures of the clusters in bacterial ferredoxins and HiPIPs are nearly identical (Backes *et al.*, 1991). However, the peptide sequences and folding patterns, the location of the cysteines, the cysteine ligand dihedral angles (close to 180° in HiPIPs), and the position of the hydrogen bonds are completely different (Adman *et al.*, 1975; Backes *et al.*, 1991). In ferredoxins, eight NH−S hydrogen bonds are present, while in HiPIPs, only five are found (Adman *et al.*, 1975; Backes *et al.*, 1991). These hydrogen bonds stabilize the more negatively charged reduced states (Adman *et al.*, 1975; Backes *et al.*, 1991; Langen *et al.*, 1992; Jensen *et al.*, 1994). By comparing bacterial ferredoxins, HiPIPs, and synthetic clusters, Carter (1977) found that each hydrogen bond increases the potential by about 80 mV. In HiPIPs, the cluster is completely inaccessible to water and surrounded by hydrophobic residues, while the ferredoxin cluster is in a more hydrophilic environment and much more accessible to

† This research was supported by the Dutch Technology Foundation (STW) as part of the Research Programme Biosensors and by a U.S. National Institute of Health grant (GM 21277).

* Corresponding author. Fax: +31 3174 84801.

‡ Agricultural University Wageningen.

§ University of Arizona.

⊗ Abstract published in *Advance ACS Abstracts,* October 15, 1995.

[1] Abbreviations: E_m, midpoint potential; HiPIP, high-potential iron−sulfur protein; NHE, normal hydrogen electrode; red, reduced; ox, oxidized; SCE, saturated calomel electrode; RGEL, *Rhodocyclus gelatinosus*; RTEN, *Rhodocyclus tenuis*; CVIN, *Chromatium vinosum*; TROS, *Thiocapsa roseopersicina*; CGRA, *Chromatium gracile*; TPFE, *Thiocapsa pfennigii*; PS, *Paracoccus* species; RSAL, *Rhodospirillum salinarum* iso-2; RGLO, *Rhodopila globiformis*; EV1, *Ectothiorhodospira vacuolata* iso-1; EV2, *Ectothiorhodospira vacuolata* iso-2; EH1, *Ectothiorhodospira halophila* iso-1; EH2, *Ectothiorhodospira halophila* iso-2; UV/vis, ultraviolet/visible.

0006-2960/95/0434-14675$09.00/0

Table 1: Redox potentials and general features of the HiPIPs

	E_m[7] (mV)	size[a]	charge[b]	number of the amino acids				surplus apolar residues
				H	W, Y, F	S, T, H, N, Q	A, V, L, I, M, P, F, Y, W	
R. gelatinosus[c]	332[d] 329[e]	74	+5	1	7	12	35	23
R. tenuis 2761[f]	302[g] 310[e]	62	+5	0	5	12	26	14
R. tenuis 3761[h]	304[g]	64	+5	0	5	16	27	11
C. vinosum[i]	356[d] 346[e]	85	−3	1	6	17	41	24
T. roseopersicina[j]	342[g]	85	−4	3	6	17	42	25
C. gracile[j]	347[h]	83	−5	2	6	16	38	22
T. pfennigii[k]	352[d]	81	−7	4	8	24	34	10
Paracoccus sp.[l]	282[d] 360[m]	71	−10	2	6	23	28	5
R. salinarum iso-2[n]	500[e]	54	+1	2	6	15	25	10
R. globiformis[o]	453[g] 432[c]	57	+1	0	4	12	22	10
E. vacuolata iso-1[p]	260[g] 259[e]	72	−3	3	6	17	32	15
E. vacuolata iso-2[p]	150[g] 172[e]	71	−6	2	7	17	32	15
E. halophila iso-1[q]	110[g] 120[r]	71	−10	4	8	13	29	16
E. halophila iso-2[s]	50[g]	76	−13	4	10	14	32	18

[a] Number of amino acids. [b] From number of Lys, Arg, Asp, and Glu. [c] Tedro *et al.*, 1976. [d] Mizrahi *et al.*, 1980. [e] This paper (pH 7.0, $I = 0.01$, and 22 °C). [f] Sequence from Tedro *et al.* (1985a) and corrected by Rayment *et al.* (1992). [g] Przyssieki *et al.* (1985). [h] Sequence from Tedro *et al.* (1979) and corrected by Rayment *et al.* (1992). [i] Sequence from Dus *et al.* (1973) and corrected by Tedro *et al.* (1981). [j] Tedro *et al.* (1981). [k] Tedro *et al.* (1974). [l] Tedro *et al.* (1977). [m] Hori, 1961. [n] Ambler *et al.*, unpublished. [o] Ambler *et al.*, 1993. [p] Ambler *et al.*, 1994. [q] Sequence from Tedro *et al.* (1985b) and corrected by Breiter *et al.* (1991). [r] Eltis *et al.*, 1994. [s] Tedro *et al.*, 1985b.

water (Backes *et al.*, 1991; Orme-Johnson *et al.*, 1983). The hydrophobic pocket in HiPIPs causes a further lowering of the reduction potentials (Kassner & Yang, 1977). These differences result in a shift of the redox potentials of both the 3+/2+ and the 2+/1+ transitions of the [4Fe-4S] cluster to such an extent that in HiPIPs the second transition, normally observed in bacterial ferredoxins, is shifted out of the biologically useful potential range while the first transition becomes feasible [*cf.* Cammack (1973), Butler *et al.* (1980), and Jensen *et al.* (1994)].

The $[4Fe\text{-}4S]^{3+/2+}$ potential ranges from +50 to +500 mV (Table 1). These large differences in redox potentials are probably caused by differences in polarity of the cluster environment and ability to delocalize electrons by the amino acid residues around the cluster (Backes *et al.*, 1991; Krishnamoorthi *et al.*, 1989). Luchinat *et al.* (1994) suggested that the peptide charge, ranging from −13 to +5 (Table 1), also modulates the redox potentials.

In this paper, we report the result of the electrochemical characterization of a number of HiPIPs by direct, unmediated electrochemistry. The charge of the peptide is shown to have a large influence on the electron transfer to the electrode. We propose a correlation between the peptide charge and the redox potentials. To probe the influence of the local cluster environment on the potential, we look at the position of the cluster charge-transfer band and try to correlate this with the thermodynamics of the redox reaction.

EXPERIMENTAL PROCEDURES

HiPIPs. We have investigated the HiPIPs from *Ectothiorhodospira vacuolata* strain β1 (iso-1 and iso-2), *Chromatium vinosum* strain D, *Rhodocyclus gelatinosus* strain 2.2.1, *Rhodocyclus tenuis* strain 2761, *Rhodopila globiformis* strain 7950, and iso-2 from *Rhodospirillum salinarum* strain ATCC 35394. The purifications have been published elsewhere (Bartsch, 1971, 1978; Ambler *et al.*, 1987, 1994; Tedro *et al.*, 1976, 1979, 1985a; Meyer *et al.*, 1990, 1994).

The isoelectric points of the reduced HiPIPs were measured by analytical thin-layer gel isoelectric focusing, performed at 4 °C in polyacrylamide gel (Serva, servalyt precotes 3−10) using an LKB 2217 Ultrophor electrofocusing unit. A Serva protein mix containing trypsinogen (pI = 9.30), lentil lectin (pI = 8.65, 8.45, and 8.15), myoglobin (pI = 7.35 and 6.85), human carbonic anhydrase B (pI = 6.55), bovine carbonic anhydrase B (pI = 5.85), β-lactoglobulin A (pI = 5.20), soybean trypsin inhibitor (pI = 4.55), and amyloglucosidase (pI = 3.50) was used to calibrate the system.

UV/Vis Spectroscopy. The UV/vis spectra of the reduced HiPIPs were obtained on an Aminco DW-2000 spectrophotometer (SLM instruments) interfaced with an IBM personal computer. The spectra were recorded at 22 ± 1 °C with split beam mode, a slit of 3 nm, and a scan rate of 2 nm/s with medium filtering. A holmium glass filter was used to calibrate the monochromator using the same slit, scan rate, and filtering. The HiPIPs were diluted to approximately 20 μM in 20 mM Hepes buffer (pH 7.0). To obtain fully reduced (*i.e.* $[4Fe\text{-}4S]^{2+}$) HiPIPs, 100 μM ascorbic acid (E_m = 58 mV; Clark, 1960) and 1 μM mediator phenazine ethosulfate (E_m = 55 mV) were added. The samples were measured against a reference cuvette with the same concentrations of buffer, ascorbate, and mediator. The positions of absorption maxima were determined after smoothing, and the values of three spectra were averaged, giving an accuracy better than 1 nm.

The protein concentrations were estimated from the maximum absorbance around 385 nm using an extinction

coefficient of 16 $mM^{-1}cm^{-1}$ (Bartsch, 1978; Przysiecki *et al.*, 1985).

Electrochemistry. We used the electrochemical cell for microscale electrochemistry described by Hagen (1989) with a removable disk of glassy carbon as the working electrode (15 mm diameter, Le Carbone Loraine type V25), a porous pin calomel reference electrode (Radiometer K-401), and a platinum counter electrode (Radiometer P-1312). The cell was flushed with wet purified argon. A 10−20 μL droplet of buffered protein solution was held between the horizontal working electrode and the tip of the reference electrode which was approximately 1 mm above the surface of the working electrode. Prior to each electrochemical measurement, the glassy carbon disk was polished firmly (Microcloth polishing cloth and 6 μm Metadi Diamond Compound spray, both from Buehler, U.S.A.), rinsed with water and with ethanol, and activated by exposing the lower part to a methane flame from a Bunsen burner for 30 s. Staircase cyclic voltammograms were recorded with an Eco Chemie Autolab 10 potentiostat, controlled by the Eco Chemie GPES software version 3.0 on a personal computer. A step of 1.22 mV was applied, and a sampling parameter $\alpha = 0.5$ (resulting in an averaging of the current during 20 ms around the center of the step) was used to obtain quasi-reversible voltammograms equal to analogue CV measurements (Seralathan *et al.*, 1987). A 220 μF condenser across the current−output of the potentiostat ($Z = 100\ \Omega$) was applied as a low-pass filter ($2\pi RC = 0.14$ s). Analogue CV measurements were performed using a BioAnalytical Systems Voltammograph CV27 with a 0.1 s filter.

The midpoint potentials were measured at a scan rate of 10 mV/s with upper and lower potential limits at least 150 mV higher and lower than the observed peak positions. The experiments were performed with 25−135 μM HiPIP in 10−20 mM Hepes buffer (pH 7.5) at a temperature of 22 ± 1 °C. The promoters were $MgCl_2$ (Merck), $ScCl_3$ (Aldrich), $EuCl_3$ (Fluka), poly(L-lysine) (MW = 3300) (Sigma), morpholin (Janssen Chimica), L-amino acids (Merck), phenol (Merck), and 4,4′-dipyridyl (Janssen Chimica).

The buffers used for the determination of the pH dependency of the midpoint potentials were 10−20 mM sodium acetate/acetic acid (Merck) at pH 4−5 or the "good" buffers (Sigma) Mes, BisTris, Mops, Hepes, Epps, Taps, BisTrisPropane, and Ches or Caps at pH 5.5−11, all titrated with NaOH or HCl.

Temperature-dependent cyclic voltammograms were obtained by submerging the cell in a thermostated water bath. The argon was passed through 2 m of copper tube (3 mm) submerged in the water bath. The temperature of the cell was measured using a thermocouple inserted into the salt bridge of the calomel electrode. The measurement was started when the internal temperature was within 1 °C of the temperature of the water bath, and the average of the temperatures at the start and at the end of the cyclic scan was used. At each temperature, a new droplet of solution and a new working electrode were used, unless the stability of the protein was sufficient to measure for a longer period of time (judged by the shape of the voltammogram and by a second measurement after resetting the temperature to a previously measured value). The temperature dependence of the calomel electrode was calculated from (Bard & Faulkner, 1980)

$$E_{SCE} = 244.4 - 0.661(t - 25) - 1.75 \times 10^{-3}(t - 25)^2 - 9.0 \times 10^{-7}(t - 25)^3 \text{ mV}$$

The ionic strength dependencies of the potentials were measured in 10−20 mM Hepes (pH 7.5), and the ionic strength was increased by addition of KCl (either by titration of one droplet or by using a new droplet and a new working electrode in case the electron transfer became sluggish). The ionic strength was calculated from the KCl concentration and the concentration of ionized buffer (as calculated from pH and pK). The protein itself, promoters, or stabilizers are not included in the calculated ionic strength.

Table 2: Characteristics of the Reduced HiPIPs

	charge[a]	pI	λ_{max}^{UV} (nm)	λ_{max}^{vis} (nm)	A^{UV}/A^{vis}
R. gelatinosus	+5	9.35	283.0	384.9	2.28 (2.31[b])
R. tenuis strain 2761	+5	9.08 9.44	283.7	382.9	1.34 (1.58[c])
C. vinosum	−2	3.90 4.13	283.2	386.5	2.51 (2.57[b])
R. salinarum iso-2	+1	5.62	281.8	393.2	2.11 (1.9[d])
R. globiformis	+1	4.59	282.6	386.0	1.74 (1.8[e])
E. vacuolata iso-1	−3	3.96 4.22	281.2	390.0	2.40
E. vacuolata iso-2	−6	3.48 3.66	282.5	376.9	2.36

[a] The charge of the peptide without cysteines or the cluster is given. The ratio of UV and vis absorbance between parentheses is the best purity index found in the literature. [b] Dus *et al.*, 1967. [c] Bartsch, 1978. [d] Meyer *et al.*, 1990. [e] Przysiecki *et al.*, 1985.

RESULTS

Characteristics of the HiPIPs. The spectra of the reduced HiPIPs are similar to the spectra of oxidized bacterial ferredoxins with a shoulder around 300 nm and one absorption band in the visible region around 385 nm (de Klerk & Kamen, 1966; Dus *et al.*, 1967; Meyer *et al.*, 1973, 1990; Bartsch, 1978; Meyer, 1985). The purity indices (ratio A^{280}/A^{385}, see Table 2) are comparable to reported values. The absorption maximum in the UV region is located at the same position for all HiPIPs; $\lambda_{max} = 282.6 \pm 0.8$ nm, but there are measurable differences between the positions of the maxima in the visible region.

The measured isoelectric points of the reduced HiPIPs are also collected in Table 2. *E. vacuolata* iso-1 and iso-2 and *C. vinosum* and *R. tenuis* HiPIPs focus in two bands, separated by 0.26, 0.18, 0.26, and 0.36 pH units, respectively. This is comparable to the lowering of the pI by 0.2 unit upon reduction as reported by Dus *et al.* (1967) for *C. vinosum* HiPIP and suggests partial oxidation of these HiPIPs during focusing. The measured isoelectric points are as expected from the calculated charge of the proteins, including the net −2 charge of the reduced cluster and cysteine ligands.

Electrochemistry. The charge of the protein has a large influence on the electrochemical response. Direct, unpromoted electrochemistry is possible with the positively charged *R. gelatinosus*, *R. tenuis*, and *R. globiformis* HiPIPs

(*R. salinarum* gives only a small anodic response during the first scan), but the negatively charged *C. vinosum* HiPIP and both *E. vacuolata* iso-HiPIPs require a positively charged promoter. This indicates that the electrostatic interactions between the protein surface and the negatively charged glassy carbon electrode are important for the electron transfer reaction. The positively charged promoter is believed to form a bridge between the negative charges (Armstrong *et al.*, 1987, 1988). However, not all of the "traditional" cationic bridging promoters are suitable in this case. Multivalent cations like Mg^{2+}, Sc^{3+}, or Eu^{3+} do not promote the response. With the aminoglycoside neomycin, a small and rather unstable response is observed. The best promoter proved to be poly(L-lysine). This indicates that the flexibility of the promoter is important. Apparently, the promoter must not only suppress Coulombic repulsion but also be able to adjust its shape to provide a good docking site for the protein on the electrode.

Other important factors for a reliable measurement of the potential are the stability (persistence) and reversibility (peak-to-peak separation) of the response. The ideal promoter not only provides a bridge between the protein and the electrode surface but also effects a reversible and stable electron transfer. However, poly(L-lysine) is not a good promoter in this sense. We observed that, for the three negatively charged HiPIPs promoted by poly(L-lysine), the response is not very stable. The peak-to-peak separation rapidly increases to above 100 mV after a few cycles. This was also observed for the unpromoted positively charged *R. gelatinosus* and *R. tenuis* HiPIPs. This might be caused by denaturing of the protein upon adsorption on the electrode, thereby blocking the electron transfer. The protein probably denatures to a flattened shape with hydrophobic interactions between the apolar residues and apolar patches on the electrode surface (Norde, 1986). This is confirmed by the observation that the stability of the response is less when the electrode is not activated but only polished, yielding a more hydrophobic surface (large contact angle with water). With this in mind, we screened a number of bifunctional (hydrophobic/hydrophilic, zwitterionic) substances for their ability to prevent or delay the irreversible denaturing of the HiPIPs by adsorption.

In combination with poly(L-lysine), morpholin proved to have a positive effect on the stability of the response. For *C. vinosum*, the optimum is 43−72 μM HiPIP with 7.7−9.2 mM morpholin and 0.67−0.8 mM poly(L-lysine). For *E. vacuolata* iso-1, 27−44 μM HiPIP with 7.7−9.2 mM morpholin and 0.67−0.8 mM poly(L-lysine) was used. For *E. vacuolata* iso-2, a protein concentration of 132 μM with 7.2 mM morpholin and 1.6 mM poly(L-lysine) gave the best stability.

The reversibility of the response (unpromoted) of *R. gelatinosus* HiPIP can be improved by addition of amino acids. The optimal response was obtained by addition of 3 mM aspartic acid to 51 μM protein. Some improvement of the response was also observed with Ala and His and to a lesser degree with Gln, Gly, and Thr. Below a level of 5 mM for aspartic acid, the response is diffusion-controlled (peak current proportional to the square root of the scan rate), but the addition of more of this amino acid causes a gradual shift of the peaks to lower potential, a decreasing peak-to-peak separation, and typically after 1 h a peak current proportional to the scan rate, indicating slow adsorption of the protein on the electrode surface without denaturing. The reversibility of the response of *R. tenuis* HiPIP also improves when amino acids are added, but the absorption phenomena are less pronounced. The optimal diffusion-controlled response was obtained with 3 mM tryptophan added to 84 μM protein. The amino acids apparently prevent denaturation at the electrode surface by intervening between the protein and the electrode, while at higher concentration, the interactions become too strong for the protein to leave the surface after electron transfer. Alternatively, at a low concentration of stabilizer, only a small amount of protein is adsorped and facilitates electron transfer by "self-mediation" (Verhagen & Hagen, 1992).

The electrochemical response of *R. salinarum* iso-2 HiPIP is extremely unstable. This is due probably to the degradation of the oxidized form (Meyer *et al.*, 1990). We found that none of the promoters nor the stabilizers morpholin or amino acids could improve the response. Only in the presence of phenol (3 mM or more) or 4,4′-dipyridyl (7 mM or more) was a reversible but not very stable response obtained (midpoint potentials equal in both cases). The peak-to-peak separations were around 70 mV in the first scan but rapidly increased. These aromatic stabilizers may bind to hydrophobic patches of the electrode, thereby delaying the adsorption of the protein. Because phenol is electrochemically active in the applied potential range, we decided to use 4,4′-dipyridyl as stabilizer. For the potential measurements, 11 mM dipyridyl and 67 μM *R. salinarum* HiPIP were applied and only the first and second scans were used.

The response of *R. globiformis* HiPIP is much more stable compared to the those of the other HiPIPs, and no promoter or stabilizer is required (Figure 1). This might be due to the almost equal amounts of positive (eight) and negative (seven) residues. The negative charges apparently prevent the denaturing of the protein on the electrode surface.

The midpoint potentials measured by us are comparable to the values reported before (Table 1). The potential of *R. salinarum* is the highest HiPIP potential ever reported and is close to the upper estimate of 480 mV, on the basis of the absorbance change upon a single addition of ferricyanide before decay of the oxidized HiPIP (Meyer *et al.*, 1990). The addition of morpholin to the negatively charged HiPIPs promoted by poly(L-lysine) or the addition of amino acids to the positively charged HiPIPs does not change the midpoint potentials significantly. This indicates that the broadening of the voltammograms is rather symmetrical, and thus, the oxidation and reduction are equally hampered by denatured protein. Poly(L-lysine) does not influence the midpoint potentials. Addition of 0.8 mM poly(L-lysine) to *R. globiformis* HiPIP has no effect on the midpoint potential nor on the peak current. Without a promoter, *C. vinosum* HiPIP gives a very low and poorly reversible response, but the midpoint potential is equal to the measured value in the presence of poly(L-lysine) and morpholin (measured at pH 4, 5.5, 7, 8, and 10.5).

pH Dependence of the Potentials. The results of the measurements of the redox potentials at different pHs are collected in Figure 2 and in Table 3. Generally, the response of the HiPIPs (reversibility, current) is independent of pH when the optimum concentrations of protein, promoters, and stabilizers are used. Only at high pH (>9) does the response

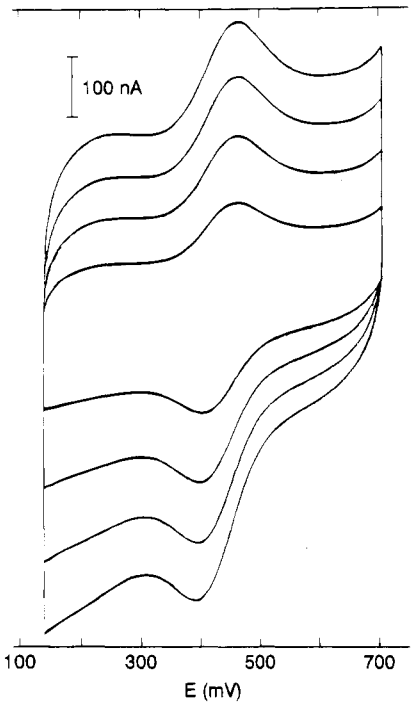

FIGURE 1: Cyclic voltammograms of 41 μM *R. globiformis* HiPIP in 16 mM Hepes (pH 7.5). A 12.5 μL droplet was used on a glassy carbon electrode activated by glowing in a methane flame. Conditions: reference/counter electrodes, SCE/Pt; scan rates, 5, 10, 15, and 20 mV/s; temperature, 22 °C. The potential axis is defined *versus* the normal hydrogen electrode. The peak currents are proportional to the square root of the scan rate with a diffusion coefficient of (8 ± 2) × 10^{-7} cm^2/s.

Table 3: Dependence of HiPIP Reduction Potentials on pH[a]

	E_m (high pH)[b] (mV)	pK_{ox}	pK_{red}	slope[c] (mV/pH)	ΔE_m (mV)
R. salinarum iso-2	500.1 ± 7.0				
R. globiformis	431.3 ± 4.5				
C. vinosum	346.5 ± 2.1	5.35	5.95	−19.3	35.0
	346.6 ± 2.1	5.65		−19.9	34.7
R. gelatinosus	312.4 ± 3.1	6.30	6.90	−19.2	34.7
R. gelatinosus + Asp	312.5 ± 2.7	6.51	7.11	−19.3	34.9
R. gelatinosus, both	312.4 ± 3.0	6.42	7.01	−19.0	34.9
	312.6 ± 3.1	6.71		−19.9	34.6
R. tenuis	309.6 ± 2.3				
R. tenuis + Trp	309.0 ± 1.2				
R. tenuis, both	308.8 ± 1.8				
E. vacuolata iso-1	257.4 ± 1.4				
E. vacuolata iso-2	166.1 ± 1.8				

[a] Results of chi-square fitting of the data with a pK_{ox} and pK_{red} and with one pK. *R. salinarum* HiPIP (67 μM) was measured in the presence of 11 mM 4,4′-dipyridyl, *R. globiformis* (58 μM) without additions, *C. vinosum* (43 μM) with 0.8 mM poly(L-lysine) and 9.2 mM morpholin, *R. gelatinosus* (51 μM) both without and with 3 mM aspartate, *R. tenuis* (84 μM) both without and with 3 mM tryptophan, *E. vacuolata* iso-1 (44 μM) with 0.67 mM poly(L-lysine) and 7.7 mM morpholin, and *E. vacuolata* iso-2 (134 μM) with 1.6 mM poly(L-lysine) and 7.2 mM morpholin, all in 10−20 mM buffer. [b] For the pH-independent potentials, the average is given. [c] The slope was calculated from the steepest part of the curve over 0.2 pH units.

of the four positively charged HiPIP become less stable and broader. The very weak response of *C. vinosum* HiPIP without promoter or stabilizer becomes stronger and more stable at low pH (4 and 5.5). At pH 4, *E. vacuolata* iso-1 gives a broad response (130 mV peak-to-peak separation) without poly(L-lysine). These observations suggest that some deprotonation occurs at high pH and some protonation of

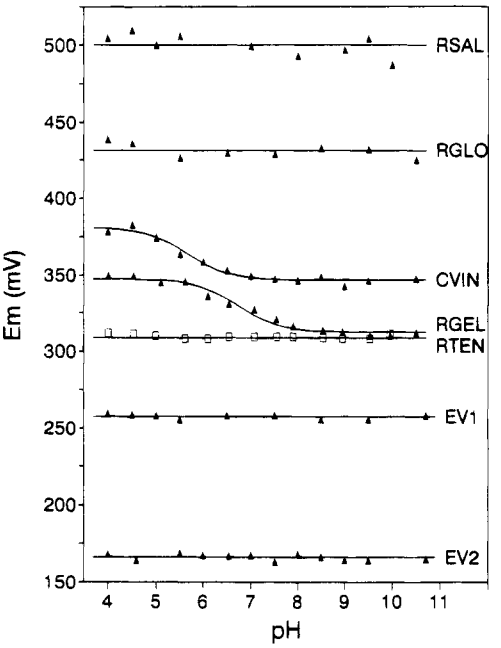

FIGURE 2: Dependence of HiPIP redox potentials on pH. Cyclic voltammograms of the HiPIPs (and promoters and/or stabilizers, Table 3) in 10−20 mM buffer were recorded at 22 °C with a scan rate of 10 mV/s: working/reference/counter electrodes, glassy carbon/SCE/Pt. The potential axis is defined *versus* the normal hydrogen electrode (*R. tenuis* is given a different symbol for clarity).

negatively charged groups occurs on the surface of either the protein or the electrode at low pH. Although 4,4′-dipyridyl is protonated around pH 6, no deterioration of the *R. salinarum* response was observed at low pH. Such a deterioration was reported for cytochrome *c* on a dipyridyl-modified gold electrode (Hagen, 1989). This indicates that, for *R. salinarum* HiPIP on glassy carbon, 4,4′-dipyridyl does not act as a hydrogen bond-accepting promoter but rather as a stabilizer.

The potentials of *C. vinosum* and *R. gelatinosus* HiPIPs both show characteristic pH−titration curves with clear plateaus at high and low pH. This indicates that the single histidine residue present in both *R. gelatinosus* and *C. vinosum* HiPIP can be titrated. The small difference between the acidic and basic potential (35 mV) and the small slopes (−20 mV/pH) can be explained by a small change of the pK upon reduction or by titration of a constant pK.

In the case of of a redox state-dependent pK, the Nernst equation for a direct redox-linked protonation can be applied to fit the data:

$$E_m = E_m{}^a + (RT/nF)\ln[([H^+] + K_{red})/([H^+] + K_{ox})]$$

in which $E_m{}^a$ is the potential at low pH. The charge of the proton influences the redox potential of the cluster, and the charge of the extra electron alters the pK of the protonation site. A difference of 35 mV between the potentials at low and high pH and a maximum slope of −19 mV/pH are obtained if the difference between pK_{red} and pK_{ox} is 0.6 unit.

When the pK is assumed to be independent of the redox state of the cluster (*i.e.* no Coulombic interaction), the effect of pH on the potentials are of an allosteric nature. Protonation of the histidine causes a change in conformation of the protein, and the altered environment of the cluster increases its potential by 35 mV. A common pH−titration

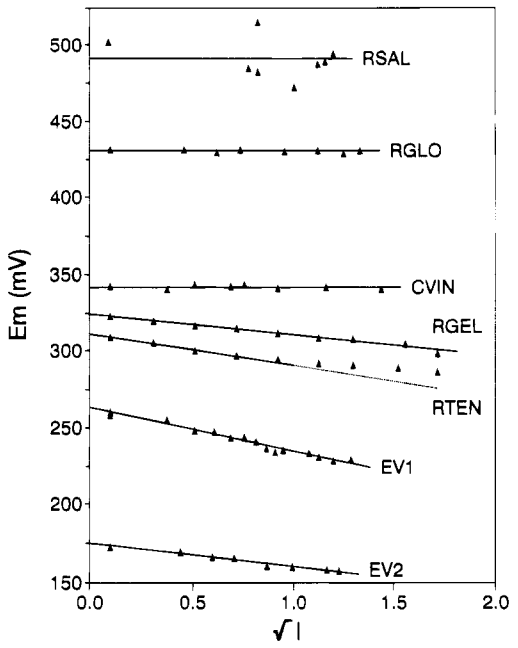

FIGURE 3: Dependence of HiPIP redox potentials on the square root of the total ionic strength. Cyclic voltammograms of the HiPIPs (and promoters and/or stabilizers, Table 4) in 10−20 mM Hepes (pH 7.5) and an increasing concentration of KCl were recorded at 22 °C with a scan rate of 10 mV/s: working/reference/counter electrodes, glassy carbon/SCE/Pt. The potential axis is defined *versus* the normal hydrogen electrode.

curve can be used to fit the data:

$$E_m = E_m{}^b + \Delta E_m/(1 + 10^{pH-pK})$$

with $\Delta E_m = E_m{}^a - E_m{}^b$, and $E_m{}^b$ is the potential at high pH. If the pK is the average of pK_{ox} and pK_{red} and the proper plateau potentials are used, the maximum slope is slightly steeper compared to the two-pK Nernst curve. However, the curves are virtually indistinguishable if the two-pK curve has pK_{red} − pK_{ox} < 1.

The results of the fits are collected in Table 3. For both *R. gelatinosus* and *C. vinosum* HiPIP, the Nernst fit yields pK_{red} − pK_{ox} = 0.6 and a pK value found with the one-pK titration formula exactly equal to the average of pK_{ox} and pK_{red}. For *R. gelatinosus*, a pK of 6.71 is found, and for *C. vinosum*, a pK of 5.65 is obtained. No significant differences of the standard deviations [=$\sqrt{(\chi^2/n)}$] are found between the one-pK fit and the Nernst fit.

Ionic Strength Dependence of the Redox Potentials. The results of the measurements of the redox potentials at different ionic strengths are summarized in Figure 3 and in Table 4. The *R. salinarum*, *R. globiformis*, and *C. vinosum* HiPIPs do not show any dependence of the midpoint potential on the ionic strength (although the data for *R. salinarum* are rather noisy due to the low stability of the electrochemical response at higher ionic strength). The potentials of *R. gelatinosus*, *R. tenuis*, and both *E. vacuolata* HiPIPs decrease with increasing ionic strength, but the dependence is not pronounced.

Generally, the stability of the electrochemical response is lower and the electron transfer kinetics slower at high ionic strength (usually above 0.5 M KCl). This is most likely due to shielding of charges and thus weakening of ionic interactions between the protein, the promoter and/or stabilizer, and the electrode surface. Hydrophobic interactions become dominant at higher salt concentrations and might cause blocking of electrode by denatured protein. It is however not likely that the measured dependence of the midpoint potential on the ionic strength is caused by asymmetrical broadening of the voltammograms due to this salt dependence of the electron transfer kinetics because the potentials are already lowered when the reversibility of the reaction is still good (peak-to-peak separation close to the theoretical 59 mV up to 0.5 M KCl).

Table 4: Dependence of HiPIP Reduction Potentials on Ionic Strength[a]

	E_m (at $I = 0$)[b] (mV)	slope (mV/√M)	r^2
R. salinarum iso-2	490.9 ± 13.1	0	
R. globiformis	430.9 ± 1.1	0	
C. vinosum	342.2 ± 1.3	0	
R. gelatinosus	323.7 ± 1.0	−14.1 ± 0.6	0.9869
R. gelatinosus + Asp	324.4 ± 0.3	−13.0 ± 0.3	0.9974
R. tenuis	311.3 ± 0.9	−21.7 ± 1.3	0.9886
R. tenuis + Trp	310.9 ± 0.2	−19.4 ± 0.7	0.9988
E. vacuolata iso-1	263.3 ± 1.8	−28.0 ± 1.3	0.9724
E. vacuolata iso-2	174.9 ± 1.0	−14.8 ± 1.0	0.9743

[a] Results of linear regression analysis of potential *versus* the square root of the ionic strength. *R. salinarum* HiPIP (67 μM) was measured in the presence of 11 mM 4,4′-dipyridyl, *R. globiformis* (58 μM) without additions, *C. vinosum* (43 μM) with 0.8 mM poly(L-lysine), and 9.2 mM morpholin, *R. gelatinosus* (51 μM) both without and with 3 mM aspartate, *R. tenuis* (84 μM) both without and with 3 mM tryptophan, *E. vacuolata* iso-1 (27 μM) with 0.8 mM poly(L-lysine) and 9.2 mM morpholin, and *E. vacuolata* iso-2 (134 μM) with 1.6 mM poly(L-lysine) and 7.2 mM morpholin, all in Hepes (pH 7.5) and KCl. [b] In case of zero slope, the average potential is given.

Temperature Dependence of the Redox Reactions. The results of the measurements of the redox potentials at different temperatures are collected in Table 5. *R. gelatinosus* HiPIP is the only HiPIP investigated by us with a clear break point in the temperature dependence. The potentials of *E. vacuolata* iso-1 and iso-2 and *R. globiformis* HiPIPs do not have break points up to 45−50 °C (measurements at higher temperatures were not possible because the small droplet evaporated too quickly under the warm argon flow). The response of *C. vinosum* HiPIP disappears at a temperature of 36 °C, although no significant broadening was observed at 29 °C. *R. tenuis* HiPIP could not be measured at 30 °C or higher without tryptophan, but with this stabilizer, a stable response was obtained up to 36 °C. *R. salinarum* HiPIP is too unstable to determine a reliable temperature dependence at all (during the adjustment of the temperature, the response disappears).

DISCUSSION

Charges, Optical Spectra, and Potentials of the HiPIPs. When the potentials and charges listed in Table 1 are compared (Figure 4), it appears that the HiPIPs can be divided into two groups. The potentials of some HiPIPs are centered closely around an average value of 333 mV, in spite of the variation of the overall charges, ranging from very negative to quite positive. This indicates that the influence of the overall charge of these HiPIPs is somehow compensated. On the other hand, the potentials of the four highly negatively charged *Ectothiorhodospira* HiPIPs are significantly lower than 333 mV and the potentials of the positively

Table 5: Dependence of the HiPIP Reduction Potentials on Temperature[a]

	intercept (mV)	slope (mV/K)	r^2	range (°C)	$\Delta S°$ (J/mol·K)	$\Delta H°$ (kJ/mol)
R. globiformis	466.9 ± 2.2	−1.59 ± 0.05	0.9921	1−49	−153.0	−86.9
C. vinosum	381.5 ± 2.2	−1.64 ± 0.09	0.9816	1−29	−158.2	−80.0
R. gelatinosus	357.0 ± 1.3	−1.59 ± 0.06	0.9959	0−29	−153.4	−76.4
	380.0 ± 1.0	−2.39 ± 0.07	0.9985	29−49	−230.2	−99.5
R. gelatinosus + Asp	357.6 ± 1.4	−1.49 ± 0.06	0.9949	0−26	−144.0	−73.8
	374.2 ± 2.6	−2.12 ± 0.17	0.9878	26−49	−204.9	−92.1
R. tenuis	344.2 ± 1.4	−1.52 ± 0.07	0.9933	0−24	−146.8	−73.3
R. tenuis + Trp	344.3 ± 1.5	−1.56 ± 0.05	0.9955	0−36	−150.3	−74.3
E. vacuolata iso-1	302.9 ± 3.1	−1.89 ± 0.05	0.9916	3−52	−182.1	−79.0
E. vacuolata iso-2	199.9 ± 2.7	−1.13 ± 0.07	0.9736	2−45	−109.4	−49.2

[a] Results of linear regression analysis of the potential *versus* the temperature, measured in 10−20 mM Hepes (pH 7.5) in an isothermal cell with a scan rate of 10 mV/s. *R. globiformis* HiPIP (68 μM) was measured without additions, *C. vinosum* (72 μM) with 0.67 mM poly(L-lysine) and 7.7 mM morpholin, *R. gelatinosus* (51 μM) both without and with 3 mM aspartate, *R. tenuis* (84 μM) both without and with 3 mM tryptophan, *E. vacuolata* iso-1 (27 μM) with 0.8 mM poly(L-lysine) and 9.2 mM morpholin, and *E. vacuolata* iso-2 (134 μM) with 1.6 mM poly(L-lysine) and 7.2 mM morpholin.

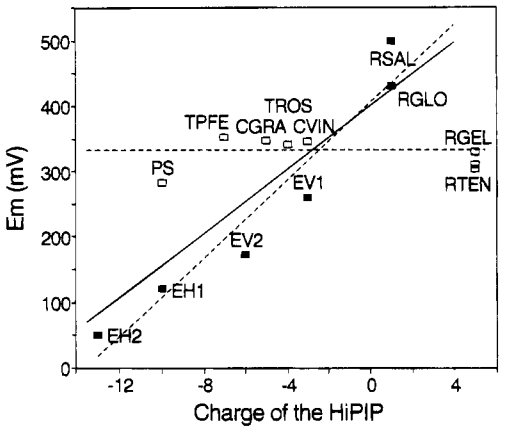

FIGURE 4: Influence of the peptide charge on the potentials of HiPIPs. The dashed lines are the average potential of the open squares (exept *Paracoccus* sp.) and the regression line for the filled squares. The solid line is the result of the chi-square refinement, including a linear dependence of the potential on the position of the absorption maximum (Figure 5).

charged *R. globiformis* and *R. salinarum* HiPIPs are higher than the average.

A lowering of the potential with increasing negative charge is expected because of destabilization of the additional negative charge in the reduced state. The simplest model for this is the linear Coulomb model. In this model, one negatively charged electron is introduced in the center of a sphere with radius r with a net charge z on the outside and a uniform dielectric constant inside this sphere. The electrostatic force on the electron is then given by

$$F = e^2 z/4\pi\epsilon\epsilon_0 r^2$$

The charge-dependent part of the reduction enthalpy is then given by the work to bring the electron from infinity into the center of the sphere:

$$\Delta h°(z) = -e^2 z/4\pi\epsilon\epsilon_0 r$$

per molecule, or

$$\Delta H°(z) = -nFE_m = -Fez/4\pi\epsilon\epsilon_0 r$$

per mole. The slope of potential *versus* charge is then

$$\delta E_m/\delta_z = e/(4\pi\epsilon\epsilon_0 rn) = 14.4/\epsilon r \quad \text{V/unit}$$

with $n = 1$, $\epsilon_0 = 8.8542 \times 10^{-12}$ C^2 N^{-1} m^{-2}, $e = 1.6022 \times 10^{-19}$ C, and r in angstroms.

When both *E. halophila* HiPIPs are included, a regression line with a slope of 29.7 ± 4.2 mV per unit charge (r^2 = 0.926 71) and a potential of 404.2 ± 53.9 mV at zero charge is obtained (dashed line in Figure 4). The *Paracoccus* HiPIP is very acidic, and the potential of 282 mV (Przysiecki *et al.*, 1985; Mizrahi *et al.*, 1980) is lower than the mean value (although Hori (1961) reported a potential of +360 mV) but not as low as would be expected from the regression line. Therefore, it may be considered to be a charge-independent HiPIP rather than a charge-dependent HiPIP. The potential and charge of *C. vinosum* HiPIP do not clearly indicate to which group this HiPIP belongs, but sequence homology with *T. roseopersicina* and *C. gracile* and similarities with *R. gelatinosus* HiPIP strongly suggest that it is a charge-independent HiPIP.

With this classification of the HiPIPs, it is possible to subtract the influence of the overall charge from the measured potentials. The remaining part of the potential then probably is a reflection of differences in the local environment of the cluster (polarity, solvation).

The relative polarity of the amino acids surrounding the cluster probably influences the UV/vis spectrum of the reduced HiPIP. In a more polar environment, the electronic state of the cluster with highest dipole moment, probably the excited state, will be lowered relative to the ground state. This results in a red shift of the absorption band (Cantor & Schimmel, 1980; Warshel & Russel, 1984). Because the electron rich reduced cluster will be more stable if it is solvated by more polar residues (Churg & Warshel, 1986), a correlation is expected between the position of the absorption band and the redox potential.

The influence of the solvation of the cluster on the visible spectrum and redox properties of iron−sulfur clusters was already observed by Hill *et al.* (1977). They examined the effect of DMSO/water mixtures on both the absorption maxima and the reduction potentials of two $[Fe_4S_4(SR)_4]^{2-}$ analogues and of *Clostridium pasteurianum* ferredoxin. By increasing the percentage of DMSO, the potentials of the analogues were lowered and the visible maximum was red shifted. The ferredoxin potential and absorption maximum did not change up to 40% DMSO, but between 40 and 80% DMSO, the maximum around 390 nm shifts to longer wavelength and the potential decreases proportionally with the percentage of DMSO.

The observed higher potential with higher percentage water is consistent with the expected stabilization of the reduced

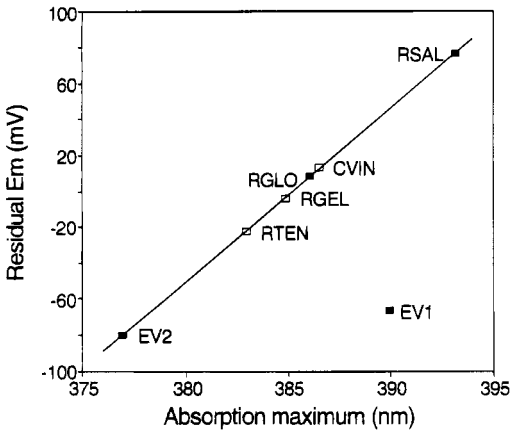

FIGURE 5: Influence of the cluster environment on the potentials of HiPIPs. Dependence of the potential on the position of the absorption band resulting from a chi-square refinement of the potentials of *R. salinarum* iso-2, *R. globiformis*, and *E. vacuolata* iso-2 with respect to the *R. gelatinosus*, *R. tenuis*, and *C. vinosum* potentials. The plotted residual potential is the redox potential of the HiPIP minus the predicted charge-dependent part of the potential (solid line in Figure 4).

state by solvation and hydrogen bonding in water, but the correlated blue shift is opposite to the expected smaller difference between the ground state and the exited state in a more polar environment. The solvent-sensitive band was ascribed to charge transfer from filled orbitals with dominant S* lone pair character to the highest occupied level with predominant tetrametal-antibonding character (Yang *et al.*, 1975). Apparently, the lone pair ground state is stabilized by the hydrogen-bonding network of water.

If the cluster pockets of the HiPIPs have different polarity but the hydrogen-bonding network to the reduced clusters are similar, this different stabilization of the ground state does not occur. A lower polarity then results in a blue-shifted absorption band and a lower potential.

Indeed, a strong linear correlation is found when the deviations of *C. vinosum*, *R. tenuis*, and *R. gelatinosus* HiPIPs from the mean potential and the deviations of the other HiPIPs from the regression line of potential *versus* charge are collected and plotted against the positions of the absorption maxima (not shown). When *E. vacuolata* iso-1 is excluded, regression yields a line with a slope of 7.01 ± 0.91 mV/nm, crossing the *x*-axis at 386.2 nm ($r^2 = 0.937\,40$). The sign of the slope is in accordance with the expected influence of polarity on the potentials and spectra. This uniform behavior of both types of HiPIPs indicates that the relative solvation of the cluster has the same effect on the potentials in all HiPIPs and apparently is independent of the influences of charges on the potential. Therefore, the modulation of the potential by charges and by the polarity of the pocket can be assumed to be additive, and the parameters can be refined by a least-squares minimization. Starting with the values obtained from the regression lines, this results in general formulas for both groups of HiPIPs:

$$E_m^{\,7} = 332.9 + (\lambda_{max} - 385.2) \times 9.661 \text{ mV}$$

for the *Chromatium*-like HiPIPs with charge-independent potentials and

$$E_m^{\,7} = 399.3 + 24.52z + (\lambda_{max} - 385.2) \times 9.661 \text{ mV}$$

for the *Ectothiorhodospira*-like charge-dependent HiPIPs. These results are plotted in Figure 4 (solid line) and in Figure 5. The standard deviation $\sqrt{(\chi^2/n)}$ of the predicted potentials from the measured potentials improved from 6.1 to 0.6 mV (*E. vacuolata* iso-1 excluded). The average potential of the charge-independent HiPIPs of 332.9 mV was not included in the minimization because it only serves as a reference point for the potential scale. From the slope of 24.5 mV per unit charge, an apparent relative dielectric constant ϵ_{app} of 84 can be calculated when an average radius of 7 Å is assumed (Dunham *et al.*, 1991; Carter *et al.*, 1974a; Freer *et al.*, 1975; Rayment *et al.*, 1992; Breiter *et al.*, 1991; Benning *et al.*, 1994). This is close to the dielectric constant of water, indicating that the influence of the charges is not only quenched by the peptide matrix but probably also by the water dipoles surrounding the charged groups at the surface (Churg & Warshel, 1986; Warshel & Russel, 1984).

Although the two *E. halophila* HiPIPs were not included in the fit, the prediction of the potentials is remarkably accurate. An additional argument to include *E. halophila* and *R. globiformis* in one group is the findings of Nettesheim and of Bertini and co-workers (Nettesheim *et al.*, 1992; Banci *et al.*, 1993a,b; Bertini *et al.*, 1992, 1993) that the electronic distribution within the oxidized clusters is in equilibrium between two forms. In one form, Cys-46 is bound to an iron(III) ion and Cys-77 to a mixed valence iron (with the iron coordinated by Cys-63), and in the other form, this is reversed. The HiPIPs from *C. vinosum* and *R. gelatinosus* have the cluster mainly in the first form (ratio 70/30 and 80/20), while *E. halophila* iso-2 and *R. globiformis* are found more in the second form (ratio 10/90 and 30/70). The cluster in *E. vacuolata* iso-2 is found in an intermediate 60/40 ratio.

The dependence of the potential of electron-transferring proteins on the net charge of the protein was already mentioned by Rees (1985). A slope of 23 mV per charge was found for the soluble one-electron carrier proteins, including HiPIPs, ferredoxins, flavodoxins, azurins, and cytochromes. However, Moore *et al.* (1986) commented that this linear correlation is fortuitous because the different types of proteins are likely to have different contributions of the bonding interactions at the redox center and conformational changes to the redox potentials, and some proteins far from the observed trend were not included. They concluded that the interactions between the redox center charge and the charges on the protein surface are relatively small compared to interactions with more buried charges. For example, it was found that ionization of a buried propionic acid residue attached to the heam lowers the potential of *Pseudomonas aeruginosa* cytochrome c_{551} by 65 mV. This was explained in terms of a local dielectric constant of 27, quenching the electrostatic repulsion of the electron (Moore, 1983; Rogers *et al.*, 1984).

With this in mind, it might be possible to explain why the potentials of a large group of HiPIPs do not depend on the charge of the peptide. The four known structures do not reveal systematic differences between the two groups in exposure of the charges to water nor in the distances to the cluster. The explanation must therefore be sought in differences in the dielectric properties of the protein matrix and specific interactions of amino acid residues with the cluster.

A large effect on the dielectrics of the protein matrix might be expected from the aromatic residues. The number of aromatic residues varies (Table 1), but some are conserved,

both in position and in orientation. From the sequences and the four known crystal structures, it is clear that Tyr-19 and the aromatic residues 76 and 80 (*Chromatium* numbering) are highly conserved and are positioned exactly between the cluster and the hydrophilic loop between Tyr-19 and Cys-43. The aromatic residues in the twisted antiparallel β-sheet (formed by parts of the peptide between the second and the last cysteine) are positioned at the opposite side of the cluster, separating it from the second hydrophilic loop (residues 51−59) (Carter *et al.*, 1974a; Freer *et al.*, 1975; Rayment *et al.*, 1992; Breiter *et al.*, 1991; Benning *et al.*, 1994). They are less conserved, but it seems that at least one must be present to complete the four-membered ring of aromatic residues located around one side of the cluster. These aromatic side chains most likely provide an apolar cluster environment in all HiPIPs and thus are responsible for the lowering of the potential relative to ferredoxin clusters. No clear differences in the structures can be found between the two groups. However, within the group of *Ectothiorhodospira*-like HiPIPs, an increasing number of aromatic residues coincides with a decreasing potential.

Table 1 also shows a correlation between the influence of the charge on the potential and the total number of apolar (A, V, L, I, P, M, W, Y, and F) and the number of uncharged polar (S, T, H, N, and Q) residues. In the group of *Chromatium*-like HiPIPs, the surplus hydrophobic residues decrease almost linearly with increasing overall charge. In the charge-dependent *Ectothiorhodospira* HiPIPs, the slight increase of this number with increasing charge probably reflects the increasing number of aromatic residues. The surplus hydrophobic residues in *R. gelatinosus* HiPIP are comparable to those of *C. gracile* with an equal but opposite charge. The relatively low number of apolar residues in the small *R. globiformis*, *R. salinarum* iso-2, and *R. tenuis* HiPIPs is probably due to a higher surface-to-volume ratio.

Interestingly, in *R. tenuis* HiPIP (strains 2761 and 3761), a buried aspartate is present at position 46 and one inserted amino acid at position 47 (Asn in strain 2761 and Ser in 3761), where most other HiPIPs have a lysine that is exposed to the solvent (Val in both *E. halophila* HiPIPs, Asp in *Paracoccus* HiPIP, and Tyr in *T. pfennigii* HiPIP). Also, the nearby Phe that is present in most HiPIPs (Val in *R. globiformis* and Tyr in *T. pfennigii*) is replaced by Ile-43 (Benning *et al.*, 1994). Apparently, the high positive peptide charge of the small *R. tenuis* HiPIP is compensated by substitution of the largely conserved "FPGK" hairpin turn between the second and third strand of the β-sheet (Carter *et al.*, 1974a) into "IPGDx", with a buried negative charge to lower the potential.

In the *Paracoccus* HiPIP, the presence of Glu-59 in the third strand of the β-sheet near the cluster coincides with a potential 50 mV lower than expected. In the *C. vinosum* structure, Asn-72 occupies this position, located next to Trp-60 in the second β-strand (Carter *et al.*, 1974a). Only in the *E. halophila* HiPIPs is a charged residue (Lys in iso-1 and Arg in iso-2) present at the equivalent position, but in these HiPIPs, the lysine in the FPGK hairpin turn is substituted by valine.

It appears that, in the *Chromatium*-like HiPIPs, an increasing peptide charge is counteracted by increasing the dielectric constant of the protein matrix. In *R. tenuis*, a buried negative charge compensates the positive charge. This "active" compensation of charges suggests that the potential of 333 mV is important for the function of these HiPIPs. The potentials of the *Ectothiorhodospira*-like HiPIPs are tuned by the peptide charge and possibly also by the number of aromatic residues around the cluster.

pH Dependence of the Potentials. At a pH between 4 and 10, protonation of histidines is most likely to cause pH-dependent midpoint potentials. As expected (Przysiecki *et al.*, 1985; Krishnamoorthi *et al.*, 1989; Luchinat *et al.*, 1994), the potentials of the two HiPIPs without histidines (*R. globiformis* and *R. tenuis*) are independent of pH. For the other HiPIPs, a difference in sensitivity to protonation of the histidines might be expected to coincide with the difference in sensitivity of the cluster to charges on the surface of the HiPIPs. However, the observed pH dependence is opposite to the predicted effect; the potentials of *C. vinosum* and *R. gelatinosus* HiPIPs are 35 mV higher at low pH, but the potentials of *E. vacuolata* iso-1 and iso-2 are not pH-dependent in spite of the three and two histidine residues present in these proteins (Ambler *et al.*, 1994). This might well be related to the different positions of the histidines.

In the *C. vinosum* and *R. gelatinosus* HiPIPs, the histidine is located directly next to the first cysteine (His-42 and Cys-43 in *Chromatium*), positioned above the plane of the aromatic residues surrounding the cluster on the pseudo-symmetry axis and, although facing toward the surface, not fully exposed to water (Nettesheim *et al.*, 1980). From the 35 mV increase of the potential upon protonation and the distance between the histidine and the cluster of about 8.5 Å in *C. vinosum*, an apparent dielectric constant of 48 can be calculated. In the two *E. vacuolata* HiPIPs, this particular histidine is not present. Instead, all histidines are located in the hydrophilic loop that connects the conserved tyrosine and the first cysteine and are fully exposed to water (Benning *et al.*, 1994). Apparently, the protonation of these histidines has no significant effect on the energy of the electron in the cluster because of shielding by the surrounding water and possibly also by the highly aromatic protein matrix between the loop and the cluster. The pH independence is probably not caused by the positive charge of poly(L-lysine); at pH 4, *E. vacuolata* iso-1 gives a very unstable and broad response (130 mV peak-to-peak separation) with an apparent midpoint potential of 280 mV. This is only 20 mV higher than the potential in the presence of poly(L-lysine) (70 mV peak-to-peak separation) and might be fully caused by asymmetrical broadening.

The potential of *R. salinarum* HiPIP is also independent of pH. Two histidines are present in this HiPIP (Ambler *et al.*, unpublished), but the sequence is too divergent from the other HiPIPs to model the structure.

The p*K* values measured for *C. vinosum* and *R. gelatinosus* are slightly lower compared to reported pH profiles (Nettesheim *et al.*, 1980, 1983; Mizrahi *et al.*, 1976, 1980; Przysiecki *et al.*, 1985). However, this is not an artifact of the promoter; aspartic acid does not significantly alter the pH profile of *R. gelatinosus* HiPIP, and the potentials of *C. vinosum* HiPIP without promoter at pH 4, 5.5, 7, 8, and 10.5 are equal to the values measured in the presence of poly(L-lysine).

Our observations differ from the pH profiles reported by Luchinat *et al.* (1994). They used an edge−plane pyrolytic graphite electrode without promoters or stabilizers. The potentials were measured with differential pulse voltammetry

(DPV), and the midpoint potentials were determined by correction of the peak position by half the pulse amplitude. The observed peaks were reported to be broadened ($n = 0.8-0.9$). Unbuffered solutions of 100−300 μM HiPIP with 0.5 M NaCl were titrated with concentrated NaOH or HCl. The results for *R. globiformis* (pH-independent), *C. vinosum* ($pK_{ox} = 6.2$ and $pK_{red} = 6.6$), and *R. gelatinosus* ($pK_{ox} = 7.2$ and $pK_{red} = 7.5$) are comparable to our observations (although they did not find clear plateaus at low pH), but pH-dependent potentials were also found for both *E. vacuolata* iso-HiPIPs. However, from our observations, it is clear that the response at a carbon surface without promoters is very unstable and the electron tranfer kinetics are very much dependent on the pH without promoters. Moreover, at higher ionic strength and with the reported high protein concentrations, the response also becomes worse. When such quasi-reversible systems are measured by DPV, the peak not only will be lower and broader but also will be significantly shifted by an activation overpotential. It is therefore possible that at least part of the dependence of the potential on pH observed by Luchinat *et al.* originates from a pH-dependent electron transfer rate. The midpoint potentials obtained with cyclic voltammetry are less sensitive to the electron transfer rate. For quasi-reversible systems, the peak-to-peak separation increases with increasing scan rate, but if the broadening is symmetrical, this does not influence the measured midpoint potential.

Thermodynamics of the Redox Reactions. At low temperature, the slopes of the E_m *versus* T plots are between −1.2 and −1.8 mV/K. These slopes are steep (large negative $\Delta S°$) compared to those of many other redox proteins (Taniguchi *et al.*, 1980), indicating that the reduced protein has a very rigid structure. The redox thermodynamics of *C. vinosum* HiPIP determined by us differ from the $\Delta H° = -66.0$ kJ/mol and $\Delta S° = -107$ J/mol·K (−1.1 mV/K) reported by Taniguchi *et al.* (1980).

The average slope of *R. gelatinosus* HiPIP changes around 28 °C from −1.5 to −2.2 mV/K. This is indicative of a change of conformation around 28 °C (Taniguchi *et al.*, 1984). The increased loss of both enthalpy ($\Delta\Delta H° = -20.7$ kJ/mol) and entropy ($\Delta\Delta S° = -69$ J/mol·K) is tentatively ascribed to the loss of a hydrogen bond in the oxidized state of *R. gelatinosus* HiPIP above 28 °C and repair of that bond upon reduction. Krishnamoorthi *et al.* (1986) concluded from the differences in the patterns of exchangeable hyperfine-shifted peaks (^{1}H-NMR) that the two *E. vacuolata* and two *E. halophila* HiPIPs have more H bonds in the reduced state than in the oxidized state. Carter and co-workers (Carter, 1973; Carter *et al.*, 1974a,b) found from the crystal structures of oxidized and reduced *C. vinosum* HiPIP that the hydrogen bond lengths are longer in the oxidized protein than in the reduced state. Therefore, it is likely that at higher temperatures the hydrogen bonds are broken more easily in the oxidized state. The extra loss of enthalpy of 21 kJ/mol above 28 °C is an acceptable value for the (re)formation of one extra NH−S hydrogen bond upon reduction (Pogorelyi, 1977; Sheridan & Allen, 1980). This means that the lowered redox potential above 28 °C is not caused by additional destabilization of the reduced state but is caused by a loss of entropy that outweighs the more favorable reduction enthalpy at these temperatures.

The unstable response of *C. vinosum* and *R. tenuis* HiPIPs at higher temperature might also be caused by the loss of a hydrogen bond and might be a general feature of all *Chromatium*-like HiPIPs. This is supported by the suggestion of Backes *et al.* (1991) that the five hydrogen bonds to the cluster in *C. vinosum* HiPIP compared to the eight hydrogen bonds in ferredoxins "represent a compromise between maximal hydrogen bonding for structural stability and minimal hydrogen bonding to achieve a higher cluster oxidation level". Thus, if a hydrogen bond is lost, the protein may unfold more readily on the electrode surface, thereby hampering the electron transfer.

A clear correlation can be found between the temperature dependence and the position of the absorption maximum. $\Delta S°$ depends linearly on the position of the absorption maximum ($r^2 = 0.964\,28$, not shown) with a slope of -5.27 ± 0.51 J·mol^{-1}·K^{-1} per nm of red shift or -16.1 ± 1.5 mV/nm at 295 K and $\Delta S°$ ($\lambda = 385.2$ nm) $= -154.7 \pm 5.0$ J·mol^{-1}·K^{-1}. All HiPIPs, including *E. vacuolata* iso-1, are reasonably close to the regression line. This indicates that the entropy loss upon reduction is influenced only by the local interaction of the cluster with the peptide in both groups of HiPIPs and not by the overall charge. Apparently, the contribution to the reduction entropy of the polarization of the water shell around the protein is small or similar for all HiPIPs. It also confirms that the charge dependence of the potential of the *Ectothiorhodospira*-like HiPIPs is fully determined by a charge-dependent reduction enthalpy, as predicted by the Coulomb model. The negative slope (more negative $\Delta S°$ with more red-shifted band) confirms that a red-shifted absorption band is an indication of a more solvated reduced cluster and thus a more ordered peptide around the cluster.

The $\Delta H°$ of most HiPIPs are between −75 and −85 kJ/mol. Only *E. vacuolata* iso-2 has a much less negative $\Delta H°$ of −51 kJ/mol. As mentioned above, the enthalpy change upon reduction is influenced both by the local polarity of the cluster environment and by the forces of the surface charges on the electron. The influence of cluster solvation on $\Delta H°$ can be calculated by subtraction of the charge-dependent part of the potential from it (a slope of −2.37 kJ·mol^{-1} per unit charge can be predicted from the 24.5 mV/unit). A combined plot of $\Delta\Delta H° = \Delta H° + 0.3329F$ against the absorption maximum for *R. tenuis*, *R. gelatinosus*, and *C. vinosum* and $\Delta\Delta H° = \Delta H° + F(0.3993 + 0.0245z)$ for *R. globiformis* and *E. vacuolata* HiPIPs (not shown) yields a straight line (when *E. vacuolata* iso-1 is not included in the regression) with a slope of -2.34 ± 0.19 kJ/mol (or $+24.2 \pm 2.0$ mV) per nm of red shift and $\Delta\Delta H°$ ($\lambda = 385.2$ nm) $= -44.8 \pm 1.5$ kJ/mol ($r^2 = 0.979\,73$). The sign of the slope (more negative $\Delta H°$ with more red-shifted absorption maximum) is consistent with the stabilization of the reduced state by polar residues. The reduction enthalpy of *E. vacuolata* iso-1 is 8.3 kJ/mol higher than expected. The resulting 86 mV lowering of the potential is, within errors, close to the deviation of −112 mV found from the fitted dependence of the potential on the peptide charge and the position of the absorption band.

When the slopes of 24.2 mV/nm for $\Delta\Delta H°$ and −16.1 mV/nm for $\Delta S°$ are combined, a slope of +8.1 mV/nm is obtained at 295 K, within errors equal to the fitted slope of the residual potentials against λ_{max}. In other words, there is a net positive shift of the potential when the polarity of the cluster environment increases. Lowering of the potential by increased ordering of the peptide is smaller (at 295 K) than

the stabilization of the reduced state by increasing solvation of the cluster. Dipolar interactions might interfere with the suggested relation between the cluster solvation and redox thermodynamics because they can either stabilize or destabilize the excited state. However, the linear relations between the position of the absorption band and the reduction entropy and enthalpy imply that the dipolar interactions with the cluster are very similar in all HiPIPs that we studied.

The potential of *E. vacuolata* iso-1 is about 100 mV too low, suggesting that the cluster is bound by one H bond less compared to the other HiPIPs (Carter, 1977). This is however not confirmed by ^{1}H-NMR (Krishnamoorti *et al.*, 1986). A different explanation for the relatively low potential of *E. vacuolata* iso-1 might be a special interaction of one or more negative charges with the cluster, destabilizing the more negatively charged reduced state. This hypothesis is consistent with the observation that the potential difference is fully determined by the less negative reduction enthalpy. However, we were not able to assign a specific residue responsible for this effect, like in *R. tenuis* and *Paracoccus* HiPIP.

Ionic Strength Dependence of the Redox Potentials. The linear relation between the redox potential and the square root or the ionic strength can be derived from the Debye–Hückel law for the dependence of the activity coefficient on ionic strength:

$$-\ln(y_i) = Az_i^2\sqrt{I}/(1 + \beta a_i I)$$

with $A = 0.5138 \ln(10) = 1.183$ (in water at 295 K), $\beta = 3.290$, the ionic radius a_i in nanometers, and ionic strength I in molarity (Lyklema, 1991). At low salt concentrations ($\leq$10 mM), this can be appoximated by

$$-\ln(y_i) = Az_i^2\sqrt{I}$$

Substitution of this limiting law into the Nernst equation leads to

$$E = E_m(I = 0) - ART/nF(z_{ox}^2 - z_{red}^2)\sqrt{I}$$

When $c_{ox} = c_{red}$ ($E = E_m$), $n = 1$, and $z_{red} = z_{ox} - 1$ at 295 K, this reduces to

$$E_m(I) = E_m(0) - 60(z_{ox} - {}^1/_2)\sqrt{I}\ \text{mV}$$

Although only the limiting law predicts this linear dependence, for the HiPIPs and also other redox proteins (Link *et al.*, 1992; Verhagen *et al.*, 1994), the linearity is extended to an ionic strength of 0.5 M or even higher. Moreover, the observed slopes are all 0 or negative, independent of the overall charge of the protein and much smaller than the Debye–Hückel theory predicts. The potential can only be independent of the ionic strength if $z_{ox} = z_{red}$. This can be accomplished by a protonation of the reduced protein. However, the potentials of *R. globiformis* and *R. salinarum* HiPIPs and (at pH 7.5) also of *C. vinosum* HiPIP are independent of both pH and ionic strength.

A partial explanation for the small slopes could be a decreasing protein radius with increasing ionic strength, resulting in a lower deviation from linearity at higher salt concentration. Specific binding of ions also cannot be excluded; Margalit and Schejter (1973) reported that the binding of chloride ions to horse heart cytochrome *c* influences the dependence of the potential on ionic strength.

In conclusion, the data suggest a subdivision of the HiPIPs into two distinct groups. The first group is formed by the *Chromatium*-like HiPIPs. These are found in *R. tenuis*, *R. gelatinosus*, *C. vinosum*, *Chromatium gracile*, *Thiocapsa roseopersicina*, and *Thiocapsa pfennigii*. The *Paracoccus* HiPIP probably also belongs to this group, although its potential is about 50 mV lower than expected. These HiPIPs have potentials around 333 mV that are modulated by the "solvation" of the cluster (hydrophilicity of the environment) as indicated by the position of the absorption maximum in the visible region of the spectrum of the reduced HiPIP. The potentials are independent of the overall charge (histidines excluded) of the HiPIPs in this group, probably because of compensation of the electrostatic forces by modulation of the polarity of the protein matrix. It is tentative to conclude from the temperature dependence of *R. gelatinosus* and the instability of *R. tenuis* and *C. vinosum* at higher temperatures that a hydrogen bond is broken at temperatures above 30 °C in all the *Chromatium*-like HiPIPs.

The second group is formed by the *Ectothiorhodospira*-like HiPIPs. The four HiPIPs from the *Ectothiorhodospira* species (although the potential of *E. vacuolata* iso-1 is about 100 mV too low) and the HiPIPs from *R. globiformis* and *R. salinarum* iso-2 HiPIP belong to this group. The potentials of these HiPIPs are strongly dependent on the overall charge (histidines excluded) of the peptide because the dielectrics of the protein matrix do not counteract the electrostatic forces. A more negative overall charge destabilizes the reduced state, resulting in a lowering of the redox potential with 25 mV per charge. The electrostatic interactions are additive to the solvating effect of the local cluster environment.

ACKNOWLEDGMENT

We are grateful to Dr. W. R. Dunham for his help in the initial phase of this research. We thank Professor Veeger for his continuous interest and support.

REFERENCES

Adman, E., Watenpaugh, K. D., & Jensen, L. H. (1975) *Proc. Natl. Acad. Sci. U.S.A. 72*, 4854–4858.
Ambler, R. P., Meyer, T. E., Cusanovich, M. A., & Kamen, M. D. (1987) *Biochem. J. 246*, 115–120.
Ambler, R. P., Meyer, T. E., & Kamen, M. D. (1993) *Arch. Biochem. Biophys. 306*, 215–222.
Ambler, R. P., Meyer, T. E., & Kamen, M. D. (1994) *Arch. Biochem. Biophys. 308*, 78–81.
Armstrong, F. A., Cox, P. A., Hill, H. A. O., Lowe, V. J., & Oliver, B. N. (1987) *J. Electroanal. Chem. 217*, 331–366.
Armstrong, F. A., Hill, H. A. O., & Walton, N. J. (1988) *Acc. Chem. Res. 21*, 407–413.
Backes, G.,Mino, Y., Loehr, T. M., Meyer, T. E., Cusanovich, M. A., Sweeney, W. V., Adman, E. T., & Sanders-Loehr, J. (1991) *J. Am. Chem. Soc. 113*, 2055–2064.
Banci, L., Bertini, I., Capozzi, F., Carloni, P., Ciurli, S., Luchinat, C., & Piccioli, M. (1993a) *J. Am. Chem. Soc. 115*, 3431–3440.
Banci, L., Bertini, I., Ferretti, S., Luchinat, C., & Piccioli, M. (1993b) *J. Mol. Struct. 292*, 207–220.
Banci, L., Bertini, I., Eltis, L. D., Felli, I. C., Kastrau, D. H. W., Luchinat, C., Piccioli, M., Pierattelli, R., & Smith, M. (1994) *Eur. J. Biochem. 225*, 715–725.
Banci, L., Bertini, I., Dikiy, A., Kastrau, D. H. W., Luchinat, C., & Sompornpisut, P. (1995) *Biochemistry 34*, 206–219.
Bard, A. J., & Faulkner, L. R. (1980) *Electrochemical methods; fundamentals and applications*, J. Wiley & Sons, New York.
Bartsch, R. G. (1971) *Methods Enzymol. 23*, 644–649.
Bartsch, R. G. (1978) *Methods Enzymol. 53*, 329–340.

Bartsch, R. G. (1991) *Biochim. Biophys. Acta 1058*, 28−30.
Benning, M. M., Meyer, T. E., Rayment, I., & Holden, H. M. (1994) *Biochemistry 33*, 2476−2483.
Bertini, I., Capozzi, F., Ciurli, S., Luchinat, C., Messori, L., & Piccioli, M. (1992) *J. Am. Chem. Soc. 114*, 3332−3340.
Bertini, I., Capozzi, F., Luchinat, C., & Piccioli, M. (1993) *Eur. J. Biochem. 212*, 69−78.
Breiter, D. R., Meyer, T. E., Rayment, I., & Holden, H. M. (1991) *J. Biol. Chem. 266*, 18660−18667.
Butler, J., Sykes, A. G., Buxton, G. V., Harrington, P. C., & Wilkins, R. G. (1980) *Biochem. J. 189*, 641−644.
Cammack, R. (1973) *Biochem. Biophys. Res. Commun. 54*, 548−554.
Cantor, C. R., & Schimmel, P. R. (1980) *Biophysical Chemistry, part II*, pp 386−389, Freeman and Co., San Francisco.
Carter, C. W. (1973) in *Iron-Sulfur Proteins* (Lovenberg, W., Ed.) Vol. III, pp 157−204, Academic Press, New York.
Carter, C. W. (1977) *J. Biol. Chem. 252*, 7802−7811.
Carter, C. W., Kraut, J., Freer, S. T., Xuong, Ng. H., Alden, R. A., & Bartsch, R. G. (1974a) *J. Biol. Chem. 249*, 4212−4225.
Carter, C. W., Kraut, J., Freer, S. T., & Alden, R. A. (1974b) *J. Biol. Chem. 249*, 6339−6346.
Churg, A. K., & Warshel, A. (1986) *Biochemistry 25*, 1675−1681.
Clark, W. M. (1960) *Oxidation-reduction potentials of organic systems*, Waverly Press, Baltimore.
de Klerk, H., & Kamen, M. D. (1966) *Biochim. Biophys. Acta 112*, 175−178.
Dunham, W. R., Hagen, W. R., Free, J. A., Sands, R. H., Dunbar, J. B., & Humblet, C. (1991) *Biochim. Biophys. Acta 1079*, 253−262.
Dus, K., de Klerk, H., Sletten, K., & Bartsch, R. G. (1967) *Biochim. Biophys. Acta 140*, 291−311.
Dus, K., Tedro, S., & Bartsch, R. G. (1973) *J. Biol. Chem. 248*, 7318−7331.
Eltis, L. D., Iwagami, S. G., & Smith, M. (1994) *Protein Eng. 7*, 1145−1150.
Freer, S. T., Alden, R. A., Carter, C. W., & Kraut, J. (1975) *J. Biol. Chem. 250*, 46−54.
Hagen, W. R. (1989) *Eur. J. Biochem. 182*, 523−530.
Hill, C. L., Renaud, J., Holm, R. H., & Mortenson, L. E. (1977) *J. Am. Chem. Soc. 99*, 2549−2557.
Hori, K. (1961) *J. Biochem. 50*, 481−485.
Jensen, G. M., Warshel, A., & Stephens, P. J. (1994) *Biochemistry 33*, 10911−10924.
Kassner, R. J., & Yang, W. (1977) *J. Am. Chem. Soc. 99*, 4351−4355.
Krishnamoorthi, R., Markley, J. L., Cusanovich, M. A., Przysiecki, C. T., & Meyer, T. E. (1986) *Biochemistry 25*, 60−67.
Krishnamoorthi, R., Cusanovich, M. A., Meyer, T. E., & Przysiecki, C. T. (1989) *Eur. J. Biochem. 181*, 81−85.
Langen, R., Jensen, G. M., Jacob, U., Stephens, P. J., & Warshel, A. (1992) *J. Biol. Chem. 267*, 25635−25627.
Link, T. A., Hagen, W. R., Pierik, A. J., Assmann, C., & von Jagow, G. (1992) *Eur. J. Biochem. 208*, 685−691.
Luchinat, C., Capozzi, F., Borsari, M., Battistuzzi, G., & Sola, M. (1994) *Biochem. Biophys. Res. Comm. 203*, 436−442.
Lyklema, J. (1991) *Fundamentals of Interface and Colloid Science, Vol. 1, Fundamentals*, Chapter 5, Academic Press, London.
Margalit, R., & Schejter, A. (1973) *Eur. J. Biochem. 32*, 492−499, 500−505.
Meyer, T. E. (1985) *Biochim. Biophys. Acta 806*, 175−183.
Meyer, T. E. (1994) *Methods Enzymol. 243*, 435−447.
Meyer, T. E., Kennel, S. J., Tedro, S. M., & Kamen, M. D. (1973) *Biochim. Biophys. Acta 292*, 634−643.
Meyer, T. E., Fitch, J., Bartsch, R. G., Tollin, D., & Cusanovich, M. A. (1990) *Biochim. Biophys. Acta 1017*, 118−124.
Mizrahi, I. A., Wood, F. E., & Cusanovich, M. A. (1976) *Biochemistry 15*, 343−348.
Mizrahi, I. A., Meyer, T. E., & Cusanovich, M. A. (1980) *Biochemistry 19*, 4727−4733.
Moore, G. R. (1983) *FEBS Lett. 161*, 171−175.
Moore, G. R., Pettigrew, G. W., & Rogers, N. K. (1986) *Proc. Natl. Acad. Sci. U.S.A. 83*, 4998−49999.
Nettesheim, D. G., Johnson, W. V., & Feinberg, B. A. (1980) *Biochim. Biophys. Acta 593*, 371−383.
Nettesheim, D. G., Meyer, T. E., Feinberg, B. A., & Otvos, J. D. (1983) *J. Biol. Chem. 258*, 8235−8239.
Nettesheim, D. G., Harder, S. R., Feinberg, B. A., & Otvos, J. D. (1992) *Biochemistry 31*, 1234−1244.
Norde, W. (1986) *Adv. Colloid Interface Sci. 25*, 267−340.
Orme-Johnson, N. R., Mims, W. B., Orme-Johnson, W. H., Bartsch, R. G., Cusanovich, M. A., & Peisach, J. (1983) *Biochim. Biophys. Acta 748*, 68−72.
Pogorelyi, V. K. (1977) *Russ. Chem. Rev. 46*, 316−336.
Przysiecki, C. T., Meyer, T. E., & Cusanovich, M. A. (1985) *Biochemistry 24*, 2542−2549.
Rayment, I., Wesenberg, G., Meyer, T. E., Cusanovich, M. A., & Holden, H. M. (1992) *J. Mol. Biol. 228*, 672−686.
Rees, D. C. (1985) *Proc. Natl. Acad. Sci. U.S.A. 82*, 3082−3085.
Rogers, N. K., Moore, G. R., & Sternberg, M. J. E. (1984) *J. Mol. Biol. 182*, 613−616.
Seralathan, M., Osteryoung, R. A., & Osteryoung, J. G. (1987) *J. Electroanal. Chem. 222*, 69−100.
Sheridan, R. P., & Allen, L. C. (1980) *Chem. Phys. Lett. 69*, 600−604.
Taniguchi, I., Iseki, M., Eto, T., Toyosawa, K., Yamaguchi, H., & Yasukouchi, K. (1984) *J. Electroanal. Chem. 174 (Bioelectrochem. Bioenerg. 13)*, 373−383.
Taniguchi, V. T., Sailasuta-Scott, N., Anson, F. C., & Gray, H. B. (1980) *Pure Appl. Chem. 52* , 2275−2281.
Tedro, S. M., Meyer, T. E., & Kamen, M. D. (1974) *J. Biol. Chem. 249*, 1182−1188.
Tedro, S. M., Meyer, T. E., & Kamen, M. D. (1976) *J. Biol. Chem. 251*, 129−136.
Tedro, S. M., Meyer, T. E., & Kamen, M. D. (1977) *J. Biol. Chem. 252*, 7826−7833.
Tedro, S. M., Meyer, T. E., & Kamen, M. D. (1979) *J. Biol. Chem. 254*, 1495−1500.
Tedro, S. M., Meyer, T. E., Bartsch, R. G., & Kamen, M. D. (1981) *J. Biol. Chem. 256*, 731−735.
Tedro, S. M., Meyer, T. E., & Kamen, M. D. (1985a) *Arch. Biochem. Biophys. 239*, 94−101.
Tedro, S. M., Meyer, T. E., & Kamen, M. D. (1985b) *Arch. Biochem. Biophys. 241*, 656−664.
Verhagen, M. F. J. M., & Hagen, W. R. (1992) *J. Electroanal. Chem. 334*, 339−350.
Verhagen, M. F. J. M., Wolbert, R. B. G., & Hagen, W. R. (1994) *Eur. J. Biochem. 221*, 821−829.
Warshel, A., & Russel, S. T. (1984) *Q. Rev. Biophys. 17*, 283−422.
Yang, C. Y., Johnson, K. H., Holm, R. H., & Norman, J. G. (1975) *J. Am. Chem. Soc. 97*, 6596−6598.

BI950753B